DIELECTRIC PROPERTIES AND CURIE-WEISS BEHAVIOUR OF $Pb(Zn_{1/3}Nb_{2/3})O_3$-$PbTiO_3$-$PbZrO_3$ CERAMICS

VLADIMÍR KOVAĽ, JAROSLAV BRIANČIN, CARLOS ALEMANY*

Institute of Materials Research,
Slovak Academy of Sciences,
Watsonova 47, 043 53 Košice, Slovak Republic
E-mail: koval@imrnov.saske.sk

**Instituto de Ciencia de Materiales de Madrid,*
Consejo Superior de Investigaciones Científicas,
Cantoblanco-280 49 Madrid, Spain
E-mail: calemany@icmm.csic.es

Received December 9, 1997.

The effects of the sintering temperature and the $Pb(Zn_{1/3}Nb_{2/3})O_3$ *content on the dielectric and piezoelectric properties of* $xPb(Zn_{1/3}Nb_{2/3})O_3$ - $(1-x)Pb(Ti_{0.53}Zr_{0.47})O_3$ *ternary system were investigated. In the case of the PZN - PZT ceramics with a low concentration of* $Zn_{1/3}Nb_{2/3}$ ($x = 0.05$)*, the values of grain size (GS), Curie temperature* (T_c)*, mechanical factor of quality* (Q_m)*, sintered density* (ρ) *and relative permittivity* (ε_r) *increase as well as maximum relative dielectric permittivity at* T_c (ε_{max})*, piezoelectric constants* (d_{33}, d_{31}) *and radial coupling factor* (k_p) *decrease with increasing sintering temperature* (T_s)*. The relative dielectric permittivity rises sharply with increasing temperature to a high peak value,* $\varepsilon_r \approx 42\ 000$*, at the phase transition temperature,* $T_c \approx 390°C$*.*

The introduction of a larger amount ($x = 0.37$) *of* $Zn_{1/3}Nb_{2/3}$ *into the system resulted in the reduced permittivity* ($\varepsilon_{max} \approx 9000$) *at the phase transition* ($T_c \approx 290$ °C) *and the broadening of the dielectric peak response. The transition temperatures are frequency dependent and shifted towards a higher temperature with increasing sintering temperatures. An extended Curie-Weiss law is observed for 0.37PZN - PZT ceramics. The coefficient of diffusivity,* $\gamma \approx 1.6 - 1.9$*, and the relative volume fraction of micro polar regions calculated from Keizer physical model are discussed from the view-point of diffuse phase transition in disordered systems. The observed lowering of the spontaneous strain as the PZN content increased has been pronounced with increasing sintering temperature and lead to the increase of the room-temperature relative permittivity,* $\varepsilon_r \approx 3200$*, and piezoelectric parameters* $d_{33} \approx 410 \times 10^{-12}$ *C N*$^{-1}$ *and* $k^p \approx 49$ *%.*

INTRODUCTION

In recent years, many tentative studies were carried out in order to improve the dielectric and piezoelectric properties of lead zirconate titanate (PZT) for the actuation function in displacement transducers, precision micropositioners and actuators. The fabrication of a PZT-based ternary solid solution consisting of the complex perovskite type compounds such as $PbA_{1/3}B_{2/3}O_3$ seems more effective than the substitution of dopants such as softeners, hardeners, and stabilisers for Pb^{2+} site or $(Zr, Ti)^{4+}$ site [1-6]. Here, A denotes a divalent cation and B a pentavalent cation. Lead zinc niobate, $Pb(Zn_{1/3}Nb_{2/3})O_3$ (abbreviated to PZN), with a perovskite structure has a rhombohedral symmetry whose lattice constants are $a = 4.061 \times 10^{-10}$ m and $\alpha = 89° 55'$ at room temperature [7]. Since lattice parameters of PZN are very close to those of PZT, it is found that solid solutions are readily formed.

Dantsiger et al. [8] reported that the relative permittivity and the piezoelectric parameters d_{31} and k^p increase on transition from binary to three- and four-component systems due to lowering of the spontaneous strain as a result of increasing lattice disorder. It is well known [9-11] that, in ABO_3-type ferroelectrics with a complex occupation of the A and/or B site in the crystal lattice are present structural and/or compositional fluctuations in a region around transition temperature. The incorporation of A-site ions and vacancies in the lattice is believed to break the long-range interaction between ferroelectrically active oxygen octahedra containing B-site cations [12, 13]. F.Li et al. [13] discussed a role of critical La content in PLZT ceramics for the destruction of long-range ferroelectric order and the formation of locally polarized regions on a nanometer scale. A nanopolar domain state has been observed in the certain composition: temperature regions in lead magnesium niobate (PMN) based solid solutions [14], $(Ba,Sr)TiO_3$ [15], etc. Cross [16] subsequently proposed that the RMS (local) polarization in relaxors has large values at temperatures well above T_c and the fluctuations in polarization P are dynamical above T_c. Therefore, the polar regions formed by the random site dipolar impurities [15] exist in the paraelectric host matrix and those are flipping in orientation as in the superparamagnet. At lower temperatures the polarization fluctuations undergo a Vogel-Fulcher-like freezing in the dielectric response [17] into a long-lived metastable condition with glass-like characteristics. In the early literature the term "diffuse phase transition" was introduced for the ferroelectric - paraelectric phase transition (FPT) accompanied by the dielectric dispersion and the broadening of dielectric peak in ferroelectric relaxors. Empirically, deviations of the dielectric permittivity from Curie-Weiss law above the phase transition may be described by the following relation [9]:

$$\frac{1}{\varepsilon_r} = \frac{1}{\varepsilon_m} + C(T-T_c)^\gamma \ , \qquad (1)$$

where $C = 1/(2\varepsilon_m\delta^2)$, and $\delta^2 = (T-T_c)^2/\{2\varepsilon_m(1/\varepsilon - 1/\varepsilon_m)\}$, and ε_r is a relative permittivity, ε_m is a maximum dielectric permittivity at transition temperature T_c, T is a temperature and γ is a measure for the degree of difuseness of FPT, ranging usually from $\gamma = 1$ (normal ferroelectric) to $\gamma = 2$ (relaxor ferroelectric).

In view of the foregoing discussion, the purpose of this investigation was to study the influence of the PZN content and the sintering temperature on the electrical properties of the PZN - PZT ternary system, which is one of the candidates for ceramic microactuator materials.

EXPERIMENTAL PART

Ceramic samples used in this study were prepared by a conventional ceramic technique. The ingredients of the desired chemical molar compositions were taken in form of oxides such as Pb_3O_4, TiO_2, ZrO_2 , Nb_2O_5 and ZnO. The weighed raw materials were mixed and milled in a glass bottle with the glass sticks as grinding media and distilled water for 24 hours. After that, the mixture was dried, crushed and calcined at 850 °C for 2 hours in an alumina crucible. The reacted material was ground and stick - milled again for 24 hours. The dried powder was pressed into disks 13 mm in diameter and about 2 mm in thickness using a hand operated hydraulic press. The green pellets were sintered for 2 hours at 1100, 1200 and 1250 °C on a PZT plate covered with an alumina crucible containing an atmosphere powder consisting of a mixture of $PbZrO_3$ and ZrO_2 powders. For poling treatment and properties measurement, the sintered disks were lapped step-by-step with SiC papers to 0.5 mm thickness. The lapped disks were cleaned with methanol using an ultrasonic cleaner. The silver paste was painted, and then fired on the major faces at 830 °C for 30 min. The samples of xPb($Zn_{1/3}Nb_{2/3}$)O_3- (1-x)Pb($Ti_{0.53}Zr_{0.47}$)O_3 ceramics were labelled as 1N1, 1N2, ... , 2N3 according to the PZN content (x) and the sintering temperature (T_s), as given in table 1.

The weight of the pellets was taken before and after sintering to determine the PbO loss. It was confirmed that, the weight loss is negligible (< 0.6 wt.%). The geometric density was calculated from the weight and volume of the disks and compared with the theoretical value. In order to determine the crystal structure and lattice, the sintered ceramic bodies were polished and chemically etched, and measurements carried out at room temperature by X-ray diffraction (XRD) method using CuK_α radiation. Kim et al. [18] reported that the (200) reflections of the X-ray diffraction patterns for the PZT solid solutions split into two for the tetragonal structure, but do not split for the rhombohedral structure. In the solid solution containing both structures, the XRD pattern is not very sharp since the diffraction lines in the coexistence region partially overlap and the (h00) peak displays the presence of a triplet [9]. The lattice parameters were determined from X-ray diffraction angles measured in the range of $2\theta < 60°$ using the least squares method. The developed ceramic microstructure was analyzed under scanning electron microscopy (SEM), Tesla BM 340. For piezoelectric characterization, the sintered samples were poled in a silicon oil bath at a temperature of 120 °C for 30 min under a dc field of 3×10^6 V m^{-1}. The dielectric permittivity before and after poling (ε^u_r, and ε^p_r , respectively) were determined from the relationship, $\varepsilon_r = C.t \ / \ \varepsilon_0.A$, where C is a capacitance measured at 1 kHz using a LCR bridge (HP 4262A), ε_0 is a permittivity of vacuum, t is a thickness and A is an electrode surface. The dielectric and piezoelectric properties of poled samples were measured after allowing a 24 hours rest following the poling procedure. The temperature dependences of the dielectric permittivity and the dielectric loss were measured at 1, 10 and 50 kHz using an automated dielectric measurement system with a low-frequency impedance analyser (HP 4192A) in the temperature range of 20 - 450 °C. The temperature was controlled to within ± 1 °C using a temperature controller. The dielectric measurements were performed during cooling at a heating rate of - 0.5 °C min^{-1} around the Curie temperature. The effective volume fraction of the material with diffuse behaviour was determined from Keizer calculation model [11] using the experimental achieved data. The dielectric parameters describing the deviations of investigated PZN - PZT system from Curie-Weiss behaviour were evaluated according to the extended quadratic law (for $\varepsilon_r > \varepsilon_\infty$) [9]. Piezoelectric measurements were carried out on the same HP LF impedance analyser model 4192A by the iterative resonance-antiresonance method [19]. The planar coupling factor, k^p, and related piezoelectric coefficients were calculated from impedance data according to IEEE Standards [20]. The piezoelectric constant d_{33} was measured at 100 Hz by a Berlincourt Piezo d_{33} - meter.

Table 1. The summary of the structural properties of xPb($Zn_{1/3}Nb_{2/3}$)O_3 - (1-x)Pb($Ti_{0.53}Zr_{0.47}$)O_3 ceramics sintered at three different sintering temperatures T_s.

system	sample	x	Ti/Zr	T_s	ρ	GS	a_T	c_T	c/a	a_R	α_R
	1N1	0.05	53/47	1100	7.30	3.0	4.021	4.139	1.029	-	-
1N	1N2	0.05	53/47	1200	7.40	3.1	4.015	4.126	1.029	-	-
	1N3	0.05	53/47	1250	7.45	3.2	4.017	4.129	1.029	-	-
	2N1	0.37	53/47	1100	7.47	1.0	4.028	4.119	1.023	4.074	89.82
2N	2N2	0.37	53/47	1200	7.70	1.2	4.028	4.115	1.022	4.072	89.57
	2N3	0.37	53/47	1250	7.68	2.1	4.052	4.093	1.010	4.066	89.95

x – PZN content; T_s – sintering temperature (°C); ρ – sintered density (× 10^3 kg m^{-3}); GS – grain size (× 10^{-6} m); a_T, c_T – tetragonal unit-cell parameters (× 10^{-10} m); c/a – tetragonal distortion; a_R, α_R – rhombohedral unit cell parameters (× 10^{-10} m, degree).

RESULTS AND DISCUSSION

Ceramic properties

The structural properties of xPZN - (1-x)PZT materials as a function of different PZN content at different sintering temperatures are collected in the second part of table 1. The density of sintered samples (ρ) as a function of sintering temperature exhibits the increase of value up to 95 % of the X-ray theoretical density for T_s = 1250 °C. Compared to the sintered and theoretical density of 0.05PZN - PZT system (1N composition), densities of samples with a large amount of PZN content (2N composition) increased probably due to the higher concentration of heavier Nb ions partially substituting the octahedral (Ti, Zr)$^{4+}$ sites. For both compositions, the grain growth was observed as the sintering temperature increased. Figures 1*a* and 1*b* show scanning electron micrographs of polished, chemically etched fracture surfaces of the 0.05PZN - PZT sample (1N system), and 0.37PZN - PZT sample (2N system) sintered at 1250 °C for 2 hours. The micrographs reveal that the addition of $Zn_{1/3}Nb_{2/3}$ significantly reduces the rate of grain growth. In order to investigate the influence of sintering temperature on the microstructure of PZN - PZT ternary system, the XRD patterns in figures 2*a*, *b* were adopted for a better comparison of the diffraction profiles. The XRD pattern of 1N composition displays a

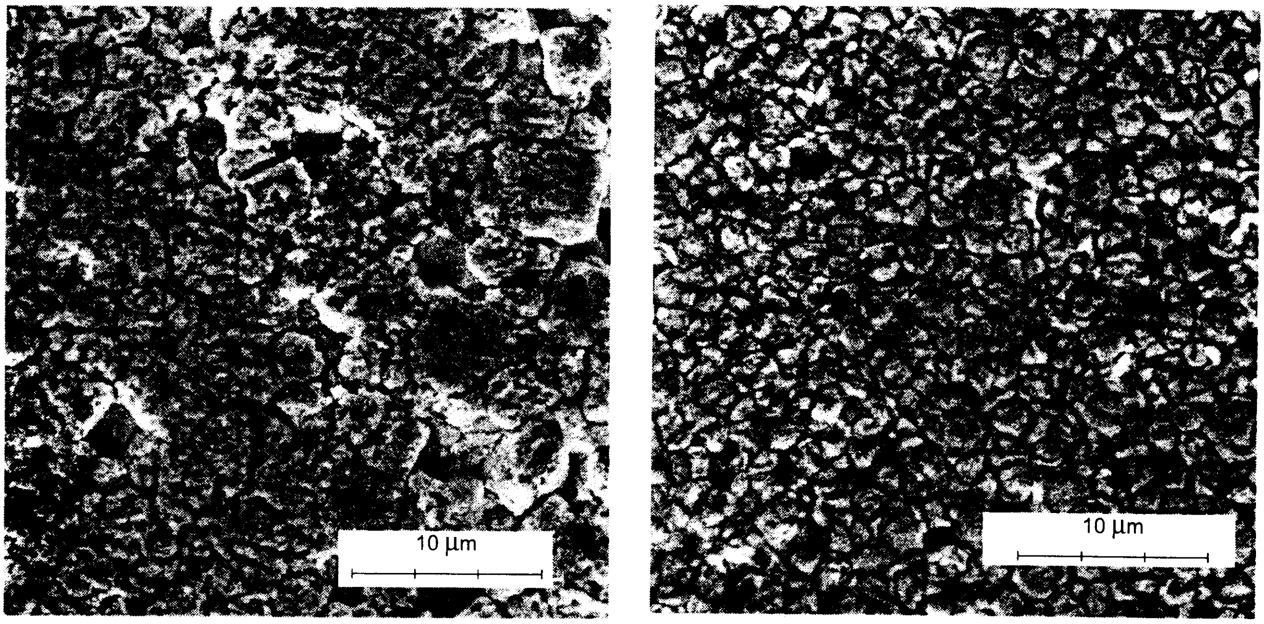

a) *b*)

Figure 1. SEM micrographs of xPb($Zn_{1/3}Nb_{2/3}$)O_3 - (1-x)Pb($Ti_{0.53}Zr_{0.47}$)O_3 ceramics sintered at 1250 °C for 2 hours.
a) x = 0.05 ; *b*) x = 0.37

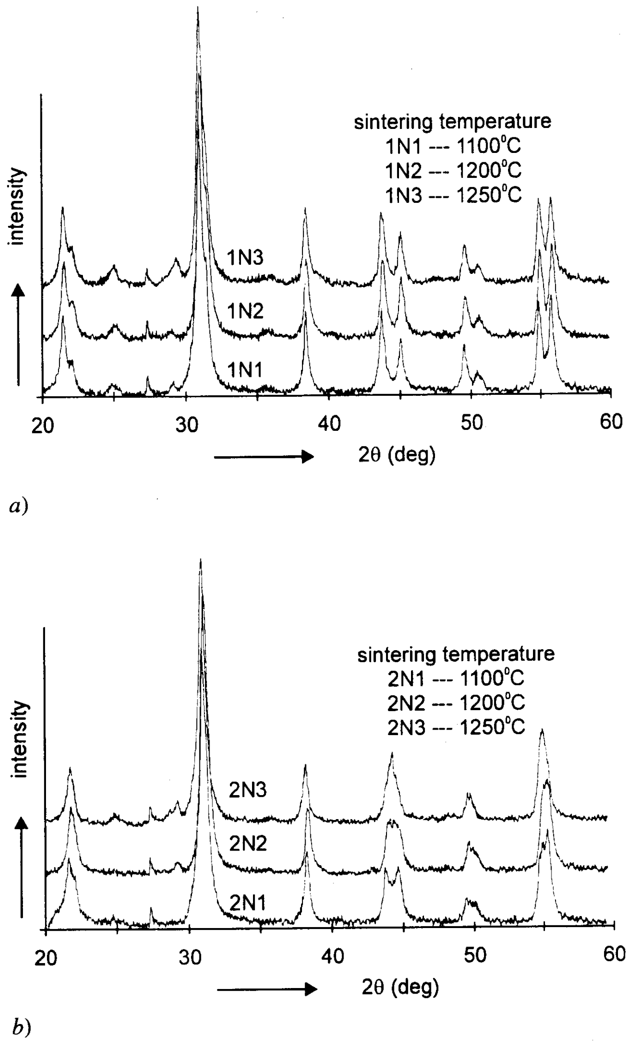

Figure 2. X-ray diffraction patterns of *a*) 0.05PZN - PZT and *b*) 0.37PZN - PZT, respectively.

tetragonally distorted perovskite structures for all temperatures of sintering. The tetragonal distortion shows no significant variations. The coexistence of tetragonal and rhombohedral phases can be seen in the PZN-rich system (figure 2*b*). In the 0.37PZN - PZT ceramics unlike to 1N system, there are visible changes of XRD patterns with sintering temperature accompanied with the different ratio of tetragonal and rhombohedral phases at the coexistence region. The increasing lattice disorder of PZN-rich system due to introduction of a large amount Nb and Zn ions into unit cells results in observed lowering of the spontaneous strain, c/a = 1.029 (1N ceramics) to 1.01 (2N ceramics). The composition of the morphotropic phase boundary for PZN - PZT system is very sensitive to variations in the sintering temperature. The results summarised in table 1 show that the tetragonal and/or rhombohedral distortion decreases as the sintering temperature increases due to compression of the tetragonal unit-cell parameter c and slight stretching of the parameter a, or shortening of the rhombohedral lattice parameter a and approaching of the crystal axis angle close to 90°, respectively.

Dielectric and piezoelectric properties

The relative permittivity and the dielectric losses before (ε^u_r, D^u) and after (ε^p_r, D^p) poling treatment of the samples with a low and high PZN concentration sintered at 3 different temperatures are listed in table 2. The results achieved from piezoelectric measurements are included in table 2, too. The dielectric permittivity after poling reaches a higher value than that before poling and the dielectric losses decrease after poling. Both phenomena can be considered as the elimination of 180° domain "clamping" effect and the reorientation of 180° domains along the poling direction. As shown in table 2, the dielectric and piezoelectric parameters increase as the sintering temperature and the $Pb(Zn_{1/3}Nb_{2/3})O_3$ content increase. It is obvious that, the ferroelectrically softer composition with a lower value of spontaneous strain exhibits increased piezoelectric and dielectric parameters. A critical role for piezoelectric properties is probably played by the space charge field of grain layer surface.

The temperature dependences of the relative permittivity and the dielectric losses for the tetragonal and morphotropic compositions of samples sintered at different temperatures are shown in figures 3*a* and 3*b* at 1 kHz measurement frequency. The character of temperature dependences was the same for the other measurement frequencies of 10 kHz and 50 kHz. One observes that the relative permittivity increases gradually with increase of temperature up to transition temperature (T_c), then it decreases. In a ferroelectric phase, the removal of the "clamping" effect for 180° domain walls by means of the thermal domain activation results in the external contribution to the dielectric permittivity. In "normal" particle size ferroelectrics represented in our study by the 0.05PZN - PZT ceramics, the domain width increases as the grain size (GS) increases, but the tetragonal distortion (c/a) remains constant. According to the increasing width, it is believed that the area of the 90° domain walls per volume strongly decreases. Therefore, the drop in the permittivity with increasing sintering temperature can be interpreted in terms of the decreasing contribution of domain walls to the relative permittivity. The relative permittivity at T_c decreases and the sharp dielectric peak shifts towards higher temperature side as the sintering temperature increases. At higher $Zn_{1/3}Nb_{2/3}$ content (x = 0.37), the reduced permittivity at T_c and the smeared-out dielectric response were observed. The diffuseness of the phase transition for relative permittivity versus temperature plots decreases with increasing sintering temperature (1100 °C onwards).

Table 2. Dielectric and piezoelectric constants for various PZN contents ($x = 0.05$ for 1N composition, and $x = 0.37$ for 2N composition) and sintering temperatures in $x\mathrm{Pb(Zn_{1/3}Nb_{2/3})O_3}$ - $(1\text{-}x)\mathrm{Pb(Ti_{0.53}Zr_{0.47})O_3}$ ceramics.

system	sample	ε_r^u	D^u	ε_r^p	D^p	σ^p	d_{33}	d_{31}	k^p	Q_m
1N	1N1	855	0.015	1008	0.011	0,355	228	-75.0	40.91	115.6
	1N2	906	0.015	1032	0.012	0.355	221	-73.3	39.31	117.7
	1N3	933	0.016	1061	0.012	0.356	215	-73.0	38.38	115.7
2N	2N1	1991	0.027	2210	0.018	0.352	360	-130	47.91	95.9
	2N2	2066	0.027	2177	0.019	0.339	409	-130	48.52	85.4
	2N3	3166	0.030	dielectric breakdown in poling treatment						

ε_r^u, ε_r^p – relative permittivity before and after poling, respectively; D^u, D^p – dielectric losses before and after poling, respectively; σ^p – planar Poisson's coefficient; k^p – planar coupling factor (%); d_{33}, d_{31} – piezoelectric coefficients ($\times 10^{-12}$ C N^{-1}); Q_m – mechanical factor of quality.

Figure 3*a* shows that, the variation of the crystal symmetry and the tetragonal - rhombohedral strain induced by the sintering temperature lead to the change of the relative permittivity at T_c. Because the spontaneous strain (*c*/*a*, table 1) decreased in PZN-rich ceramics, we consider a more complex nanopolar domain configuration responsible for the variations of the volume and domain contributions to the relative permittivity below the Curie temperature. Figures 4*a* and 4*b* contrast the dielectric permittivity and loss data for 1N3 and 2N3 ceramic samples in cooling measurements at frequencies of 1, 10 and 50 kHz. Since the permittivity curves of low PZN concentration composition show no significant frequency dependence, the 1N state can be considered a long-range ferroelectric at the whole temperature range. On the other hand, the PZN-rich samples showed a typical relaxor dielectric behaviour of disordered perovskite structures with a strong frequency dispersion at temperatures below T_c. The dielectric losses are strongly frequency dependent below the Curie temperature and much higher than that above the phase transition, too. The increasing of loss factor at T_c and the dielectric dispersion suggest that the transition from ferroelectric to the paraelectric phase is a diffuse phase transition. In addition, the transition temperature exhibits a shift towards a higher temperature with increasing frequency. The increase of the $Zn_{1/3}Nb_{2/3}$ content and the sintering temperature resulted in the increased values of dielectric losses. The temperatures corresponding to the peak in permittivity (T^1) and the peak in loss (T^2) are coincided for 1N ceramics (x = 0.05). On the contrary, in 0.37PZN - PZT samples the freezing-out temperatures are not coincident ($T^2 < T^1$) and the temperature difference is a function of measuring frequency (ΔT = 25 °C at 50 kHz). From Vogel-Fulcher law, it is well known that in dipolar as well as spin-glass system, the dielectric loss peak occurs around the inflection point bellow the temperature of dielectric permittivity peak due to the temperature dependent relaxation processes below the Curie temperature. All our dielectric measurements indicate a dipole-glass-type behaviour of 0.37PZN - PZT ceramic system with a typical relaxor state containing polar region on a nanometric scale.

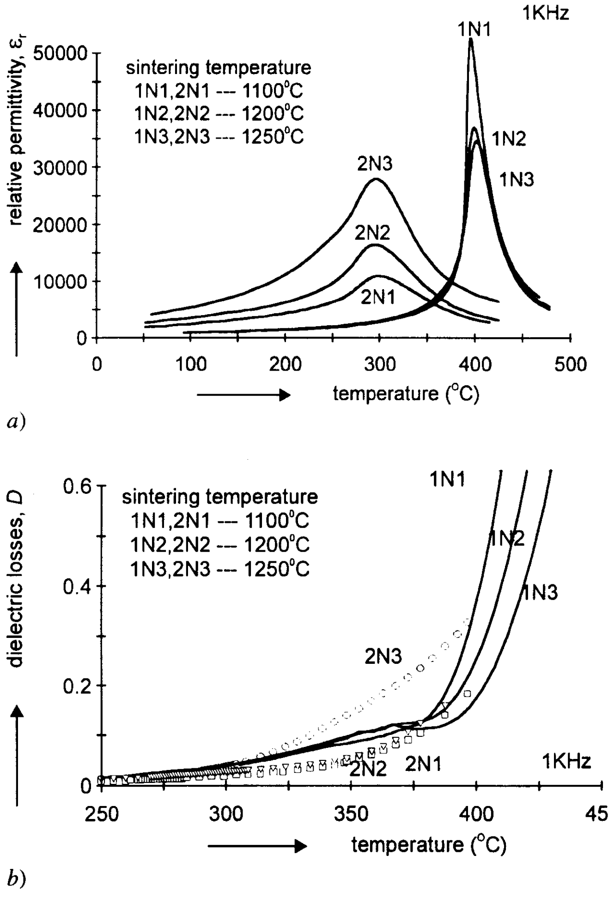

a)

b)

Figure 3. Temperature dependences of *a*) the relative permittivity (ε_r) and *b*) the dielectric losses *D* measured at 1 V_{rms} kHz^{-1} in 0.05PZN - PZT (1N) and 0.37PZN - PZT (2N) ceramic samples sintered at 1100, 1200 and 1250 °C.

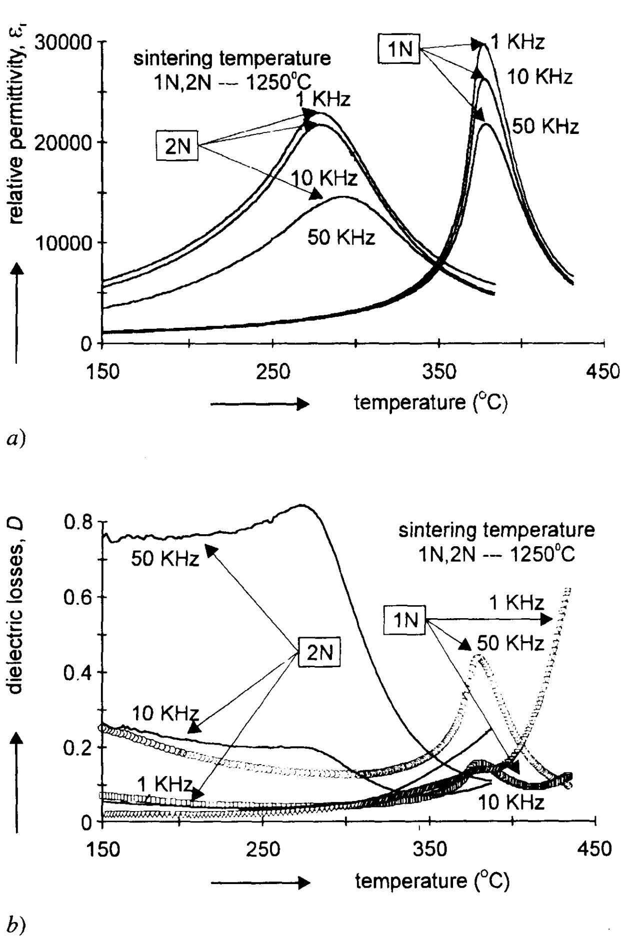

Figure 4. Temperature dependences of *a*) the relative dielectric permittivity (ε_r) and *b*) the dielectric losses at 1, 10, 50 kHz measured during cooling cycles for 1N (x = 0.05) and 2N (x = 0.37) ceramics.

The examination of diffuseness in samples has been carried out from the plot of reciprocal dielectric permittivity versus temperature for different compositions (1N and 2N) and sintering temperatures (1N1, 1N2, ... , 2N3).

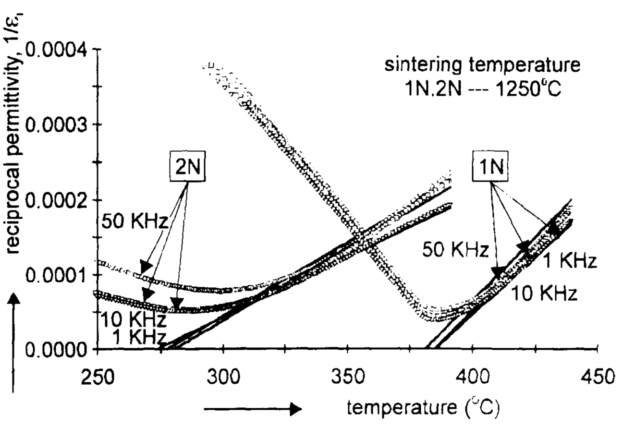

Figure 5. Behaviour of $1/\varepsilon_r$ as a function of temperature for 1N and 2N compositions at 1, 10 and 50 kHz.

The dependences exhibited similar behaviour, hence data for 1N and 2N ceramics sintered at 1250 °C are shown as representative in figure 5. The Curie-Weiss constant C_{cw}, the Curie-Weiss temperature T_0 and the transition temperature T_c were evaluated in accordance to Curie-Weiss law above the Curie point and the values for 1N2 and 2N2 samples are collected in table 3. The difference between the Curie - Weiss temperature and the transition temperature $\Delta T = |T_c - T_0|$ as well as the Curie-Weiss constant increase with increasing sintering temperature and the frequency. In the 1N set of ceramics, the broadening ΔT does not show any appreciable scatter with sintering and/or frequency, and it varies just from 1 to 5 °C.

Figure 6 illustrates the variation of $\ln(1/\varepsilon_r - 1/\varepsilon_{max})$ as a function of $\ln(T - T_{max})$ for 2N ceramic samples sintered at 1250 °C at three frequencies of measurement (1, 10 and 50 kHz). Considering the extended Curie-Weiss law (equation(1)), the values of the exponential coefficient γ were obtained from a slope of the graph of ln $(1/\varepsilon_r - 1/\varepsilon_{max})$ plotted against $\ln(T - T_{max})$. To describe the relation between the diffusivity γ and the volume

Table 3. Various parameters involved in the extended Curie-Weiss law and Keizer physical model for selected 1N and 2N ceramic samples at various frequencies.

sample	f	T_c	T_0	C_{cw}	ε_{max}	γ	v	δ
	1	386.0	387.8	2.83	29465	1.58	0.62	8.8
1N2	10	386.8	391.0	3.32	26002	1.57	0.48	10.7
	50	387.6	392.1	3.59	20606	1.66	0.36	11.8
	1	285.5	286.7	2.79	13578	1.89	0.11	33.5
2N2	10	286.0	290.0	3.05	13099	1.89	0.09	33.7
	50	286.9	292.6	3.07	9938	1.91	0.09	48.7

f – measurement frequency (× 10^3 Hz); T_c – transition temperature (°C); T_0 – Curie temperature (°C); C_{cw} – Curie-Weiss constant (× 10^{-8} °C^{-1}); ε_{max} – maximum relative permittivity; γ – diffusivity; v – volume fraction of ferroelectric material; δ – broadening of dielectric peak (°C).

fraction of ferroelectric material v in a mixture of ferroelectric (polar) and paraelectric (non polar) regions, the Keizer physical model [11] has been used. The agreement between experimental and calculated data (Keizer's model) achieved at any temperature in the paraelectric phase is representively shown in figure 7 for 0.05PZN - PZT and 0.37PZN - PZT ceramic material sintered at 1250 °C for 2 hours. The values of v are collected together with γ-coefficients in the second part of table 3. It can be seen that, the increasing of polar phase in a paraelectric matrix with the $Zn_{1/3}Nb_{2/3}$ concentration leads to the broadening of dielectric peak and the increasing of diffusivity represented by the values of δ and γ, respectively. The rise in γ and δ with an increase in frequency suggests that the broadening effect on the phase transition is more pronounced at higher frequencies when the volume fraction of dynamically disordered micro polar regions at temperatures above the Curie point increases by disturbing of thermal motion.

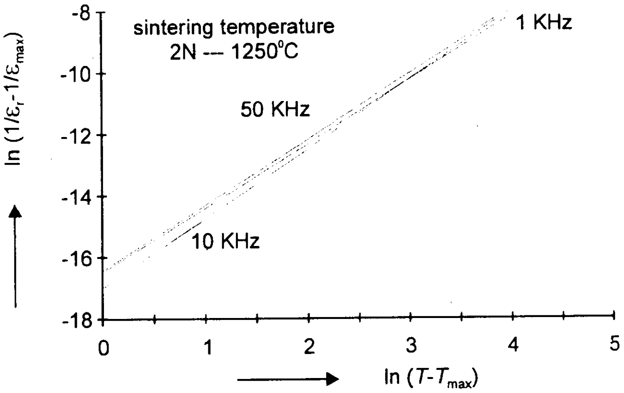

Figure 6. Plot of ln ($1/\varepsilon_r$ - $1/\varepsilon_{max}$) against ln (T - T_{max}) at three frequencies for 0.37PZN - PZT ceramic sample sintered at 1250 °C.

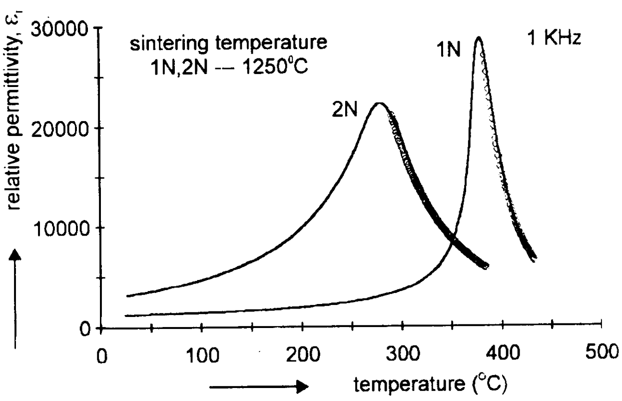

Figure 7. The calculated and measured values of the relative permittivity (ε_r) at 1 kHz for 0.05PZN - PZT and 0.37PZN - PZT ceramics sintered at 1250 °C as a function of the temperature (—— measured, OOO calculated).

CONCLUSION

The dielectric and piezoelectric properties of xPb($Zn_{1/3}Nb_{2/3}$)O_3 - (1-x)Pb($Ti_{0.53}Zr_{0.47}$)O_3 ceramics were investigated as a function of the PZN content and the sintering temperature by SEM, dielectric techniques and piezoelectric spectroscopy. The investigation lead to the following conclusions:

1. In the tetragonal structured PZN - PZT ceramics with a low $Zn_{1/3}Nb_{2/3}$ content (x = 0.05), the normal dielectric behaviour has been observed for the temperature dependence of dielectric permittivity and losses. The relative permittivity and the dielectric losses decrease as the sintering temperature increases due to the grain size effect on the twinning. The peak of the dielectric permittivity is sharp and it was shifted to higher temperature side as the temperature of sintering increased.
2. The relaxational properties of the PZN-rich ceramics (x = 0.37) were found and discussed. The increasing of the PZN content resulted in lowering grain size and spontaneous strain. The tetragonal distortion further decreased with sintering temperature and, hence the dielectric permittivity increased. The substitution of (Zr, Ti) by $Zn_{1/3}Nb_{2/3}$ causes a diffuse phase transition from the ferroelectric phase to the paraelectric phase. The transition temperature shows a shift towards a lower temperature and the smearing of the relative permittivity versus T plots increases with decreasing sintering temperature. The presence of dynamically disordered nanopolar clusters which are freezing-out at lower temperatures in a glass-like Vogel-Fulcher freezing in the dielectric response has been indicated by the observed frequency dependence of the dielectric permittivity and losses.

Acknowledgement

The authors wish to thank Mr. J. Mihalik and Mrs. K. Ďurišinova for assistance in SEM and XRD measurements. This work was supported by the Grant Agency of the Slovak Academy of Sciences GAT, Project no: 95/5303/643.

References

1. Zhu X., Meng Z.: J. Mater. Sci. *31*, 2171 (1996).
2. Nadoliisky M.M., Vassileva T.K., Vitkov P.B.: Ferroelectrics *129*, 141 (1992).
3. Wu L., Liang Ch.K., Shieu Ch.F.: J. Mater. Sci. *26*, 4439 (1991).
4. Moon J.H., Jang H.M.: J. Mater. Res. *8*, 3184 (1993).
5. Yoon S.J., Yoo S.T., Moon J.H., Jung H.J.: J. Mater. Res. *11*, 348, (1996).

6. Wi S.K., Kim H.G.: Jpn. J. Appl. Phys. *31*, 9A, 2825 (1992).
7. Kanagae T., Sakata K., Takenaka T.: Jpn. J. Appl. Phys. *30*, 9B, 2232 (1991).
8. Dantsiger A.Ya., Dergunova N.V., Dudkina S.I., Fesenko E.G.: Ferroelectrics *132*, 213 (1992).
9. Arora A.K., Tandon R.P., Masingh A.: Ferroelectrics *132*, 9 (1992).
10. Yadav K.L., Choudhary R.N.P.: J. Mat. Sc. Lett. *12*, 1722 (1993).
11. Keizer K., Lansink G.J., Burggraaf A.J.: J. Phys. Chem. Solids *39*, 59 (1978).
12. Dai X., Xu Z., Viehland D.: J. Am. Ceram. Soc. *79*, 1957 (1996).
13. Li J.F., Dai X., Chow A., Viehland D.: J. Mater. Res. *10*, 926 (1995).
14. Cross L.E.: Jpn. J. Appl. Phys. Part 1, *34*, 5B, 2525 (1995).
15. Singh N., Pandey D.: J. Phys.:Condens. Matter *8*, 4269 (1996).
16. Cross L.E.: Ferroelectrics *76*, 241 (1987).
17. Tagantsev A.K.: Phys. Rev. Lett. *72*, 1100 (1994).
18. Kim J.S., Yoon K.H.: J. Mater. Sci. *29*, 809 (1994).
19. Alemany C., González A.M., Pardo L., Jiménez B., Carmona F., Mendiola J.: J. Phys. D.: Appl. Phys. *28*, 945 (1995).
20. IEEE Standard on Piezoelectricity, ANSI/IEEE Std 176 (1987).

Submitted in English by the authors.

DIELEKTRICKÉ VLASTNOSTI A CURIE-WEISSOVE SPRÁVANIE SA $Pb(Zn_{1/3}Nb_{2/3})O_3$-$PbTiO_3$-$PbZrO_3$ KERAMIKY

VLADIMÍR KOVAĽ, JAROSLAV BRIANČIN, CARLOS ALEMANY*

Ústav materiálového výskumu,
Slovenská Akadémia Vied,
Watsonova 47, 043 53 Košice, Slovenská republika
E-mail: koval@imrnov.saske.sk

**Instituto de Ciencia de Materiales de Madrid,*
Consejo Superior de Investigaciones Científicas,
Cantoblanco-280 49 Madrid, Spain
E-mail: calemany@icmm.csic.es

V práci bol študovaný vplyv $Pb(Zn_{1/3}Nb_{2/3})O_3$ (PZN) zložky a teploty spekania na dielektrické a piezoelektrické vlastnosti $xPb(Zn_{1/3}Nb_{2/3})O_3$ - $(1\text{-}x)Pb(Ti_{0.53}Zr_{0.47})O_3$ keramiky, ktorá v súčasnosti nachádza široké uplatnenie v elektroaktívnych senzoroch a aktuátoroch, kde priama premena elektrického poľa na elastickú deformáciu sa využíva v aktuátorových elementoch a premena elastického napätia na elektrickú polarizáciu v senzoroch.

Výsledky predloženej práce ukazujú, že v prípade vzoriek ternárneho systému $xPb(Zn_{1/3}Nb_{2/3})O_3$ $\text{-}(1\text{-}x)Pb(Ti_{0.53}Zr_{0.47})O_3$ s nízkym obsahom PZN zložky ($x = 0.05$), pripravených klasickou keramickou technikou, ide o normálne feroelektriká s tetragonálnou štruktúrou. Relatívna permitivita a dielektrické straty vzoriek 0.05PZN - PZT systému klesajú so zvyšovaním teploty spekania v dôsledku ľahšej doménovej tvorby s nárastom zrna. Pík dielektrickej odozvy je ostrý a posúva sa smerom k vyšším teplotám s teplotou spekania. Súčasne so zvyšovaním teploty spekania relatívna permitivita v $T_c \approx$ 390 °C ($\varepsilon_{max} \approx$ $\approx$ 42 000), piezoelektrické konštanty ($d_{33} \approx 220 \times 10^{-12}$ C N^{-1}, $d_{31} \approx -72 \times 10^{-12}$ C N^{-1}) a väzbový faktor v radiálnom móde ($k^p \approx 40$ %) klesajú.

Zavedenie väčšieho množstva $Pb(Zn_{1/3}Nb_{2/3})O_3$ ($x = 0.37$) do binárneho $PbTiO_3$ - $PbZrO_3$ systému viedlo k zmene kryštalografickej symetrie výslednej štruktúry, v ktorej koexistujú tetragonálna a romboedrická fáza, zjemneniu mikroštruktúry a zníženiu spontánnej deformácie. Tetragonálna, resp. romboedrická deformácia ($c/a \approx 1.023$) sa so zvyšovaním teploty spekania ďalej znižovala, čo v konečnom dôsledku viedlo k pozorovanému nárastu relatívnej permitivity ($\varepsilon_r \approx 3200$) meranej pri 1 V_{rms}/1 kHz a izbovej teplote. Vysoká koncentrácia $Zn_{1/3}Nb_{2/3}$ v tomto prípade mala za následok zníženie maximálnej permitivity ($\varepsilon_{max} \approx 9000$) v bode fázového prechodu ($T_c \approx 290$ °C) a rozšírenie píku dielektrickej odozvy. Teplota fázových prechodov u vzoriek tohto systému je frekvenčne závislá a posúva sa do oblasti vyšších teplôt so zvyšovaním teploty spekania. Na určenie difúznosti fázového prechodu ($\gamma \approx 1.6$ - 1.9) a relatívneho objemového podielu mikropolárnych oblastí (≈ 0.1 - 0.6) bol v prezentovanej práci využitý rozšírený Curie-Weissov zákon a Keizerov fyzikálny model pre relaxačné feroelektriká. Vzorky so zložením blízko morfotrópnej fázovej hranice a vysokou koncentráciou PZN zložky vykazovali na rozdiel od vzoriek 0.05 PZN - PZT systému okrem vyšších dielektrických parametrov aj pre elektroaktívne senzory a aktuátory požadované lepšie piezoelektrické vlastnosti ($d_{33} \approx 410 \times 10^{-12}$ C N^{-1}, $k^p \approx 50$ %), pričom elektromechanické parametre sa postupne zvyšovali s teplotou spekania.